JPhys Energy

PERSPECTIVE

Curing perovskites—a way towards control of crystallinity and improved stability

Tobias Seewald, Emilia R Schütz, Carola Ebenhoch and Lukas Schmidt-Mende[1]

Department of Physics, University of Konstanz, D-78457 Konstanz, Germany

[1] Author to whom any correspondence should be addressed.

E-mail: Lukas.Schmidt-Mende@uni-konstanz.de

Keywords: perovskite, solar cell, methylamine, grain boundaries, stability, upscaling

Supplementary material for this article is available online

Abstract

Power conversion efficiencies of lead halide perovskite solar cells have rapidly increased in the decade since their emergence, reaching 25% this year. However, reliable film uniformity and device stability remain hard to achieve and often require precise compliance with complicated protocols, which hampers upscaling towards industrial applications. Here, we explore the potential of an alternative route towards high-quality perovskite films: The reaction between a pre-existing perovskite film and methylamine (MA) gas has been shown to possess the striking ability to both improve film morphology and increase grain size drastically, boosting device performance. This post-deposition treatment could provide the means to decouple film quality from the initial deposition process, thus promising to facilitate upscaling and lowering production costs. Furthermore, such MA gas treatments show great promise regarding the stability of fabricated devices, as they open up the opportunity to reduce or even eliminate the adverse role of grain boundaries in film degradation.

1. Introduction

With the global energy consumption ever rising while solar photovoltaics currently contributes only 2.4% of the world's electricity [1], developing innovative technologies to further accelerate a sustainable energy infrastructure is one of mankind's most pressing challenges. One of the most promising candidates of the last years are metal halide perovskites, a class of crystalline materials of the form ABX_3, where X is a halogen anion, B is a divalent metal cation (predominantly Pb^{2+} or Sn^{2+}), and A is a singularly charged cation, which may be either a small organic molecule such as methylammonium ($CH_3NH_3^+$) or formamidinium ($HC(NH_2)_2^+$), a comparably sized elementary cation like Cs^+, or mixtures thereof. Since their first reported application as a photovoltaic absorber in 2009 [2], rapid evolution of processing technique, cell architecture, and material composition have skyrocketed power conversion efficiencies (PCE) of perovskite solar cells (PSC) beyond 25% within a decade [3]. A combination of various favorable opto-electronic properties has been identified enabling efficient charge generation and extraction, i.e. high and steep-edged absorption coefficient, tunable band gap across the visible, long lifetimes and diffusion lengths of photogenerated charge carriers, and a high tolerance of the electronic characteristics towards crystallographic defects.

The latter, along with the low forming energies involved in the crystal chemistry, allows comparably facile processing at or near ambient conditions from solution, readily yielding semiconductor thin films at a fraction of the production cost of conventional high-purity wafer or epitaxy based technologies. However, on the flip side of facile and flexible film formation stand the well-known issues of reproducibility and stability, as the resulting film quality is highly sensitive to nearly all environmental and instrumental parameters, both during fabrication as well as characterization [4]. While a myriad of methodologies have been developed in the attempt to reign in the wide ranging diversity of crystalline morphologies which may emerge from their solute precursors [5],

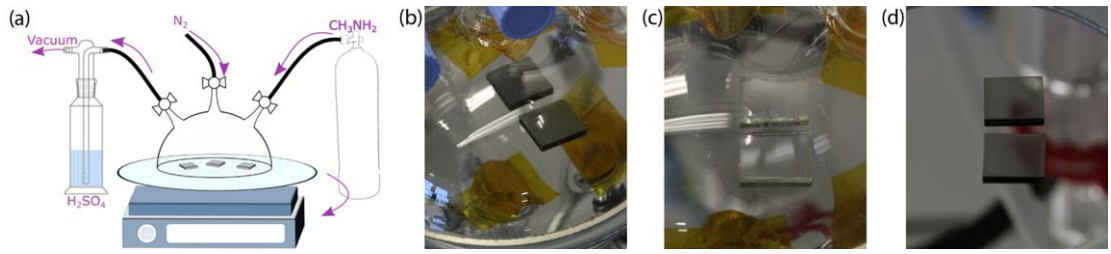

Figure 1. (a) Setup schematic for MA treatment. Photographs of (b) initial $MAPbI_3$ films, (c) transparent phase during MA exposure, (d) recrystallized films.

pushing small area device performance on its fast-paced rise, most of them rely on a highly confined parameter space, restricting them to lab-scale geometries with little applicability for industrial processes.

One concept to overcome these challenges is to decouple the final properties of the film relevant to device performance from its initial deposition via post-processing. In particular, here we want to highlight the possibilities of post-deposition treatment of methylammonium lead iodide ($CH_3NH_3PbI_3$, $MAPbI_3$) films with methylamine (CH_3NH_2, MA) gas. In this approach first described by Zhou *et al* in 2015 [6], the MA molecules intercalate the perovskite, breaking up the crystal structure and reversibly transforming the material into an intermediate liquid, transparent phase (1). Upon release of the MA gas, the previously deposited material recrystallizes, assuming the opaque perovskite form again

$$CH_3NH_3PbI_3\ (s) + x\ CH_3NH_2\ (g) \quad \rightleftarrows \quad CH_3NH_3PbI_3 \cdot x\ CH_3NH_2\ (l). \tag{1}$$

Beyond the treatment of pre-existing films, gaseous methylammonium has been used in different ways for the formation of $MAPbI_3$. Films have been fabricated through the reaction of MA gas with a precursor PbI_2-lattice [7] or a $HPbI_3$ precursor layer [8, 9], the latter producing films with remarkable stability against moisture [9].

In another application of a gas–solid reaction for perovskite-film formation, a fully formed $MAPbI_3$-film was converted to formamidinium lead triiodide ($FAPbI_3$) via exposure to gaseous formamidine ($HC(NH)NH_2$, FA) [10]. As this method has been shown to preserve the morphology of the initial $MAPbI_3$ film, it presents the intriguing possibility to directly transfer the extensive knowledge about $MAPbI_3$ film formation that has been accumulated over the past years to the formation of smooth, highly crystalline $FAPbI_3$ perovskite films.

Various other possibilities of perovskite film formation using MA and other hydrogen halide gases have been studied [11, 12], highlighting the broad applicability of this field of research.

2. Morphological control

Figure 1 shows an exemplary implementation of the MA treatment for a PSC device stack deposited up to the perovskite layer. The samples are sealed in a chamber where the partial pressure of the MA gas can be controlled via evacuation, flushing with inert gas, and an inlet for a certain amount of MA. By heating the bottom of the chamber, the substrate temperature can be defined and used to initiate recrystallization by desorbing the MA back out of the film. Alternatively, removing the MA atmosphere through the exhaust and purging with nitrogen effectuates a diffusive low-temperature outgassing, equally returning the film to its solid state.

The degree to which the MA penetrates the bulk perovskite material, and thus changes its morphology, depends on the partial pressure of the MA gas: While even macroscopic single crystals can be fully interfused [6], control of the vapor pressure dictates how complete the transition is before recrystallization [13].

Due to the 'melting'-like intermediate phase, subjected to the corresponding hydrodynamics, a smooth and compact film is formed, where contingent pinholes are closed, avoiding shunting contacts between the charge selective layers of the solar cell and thus improving the fill factor [14, 15].

As one of the most promising capacities of this method, the resulting film morphology has proven independent of the initial one, rendering previously needle-like microstructures and smooth, dense layers virtually indistinguishable after undergoing MA treatment at the same recrystallization parameters (supporting figures S1, S2 are available online at stacks.iop.org/JPENERGY/2/021001/mmedia). Thus, film morphology is primarily determined by the conditions at which the recrystallization of the perovskite takes place, decoupling it from the preceding material deposition and therefore lifting the dual requirement of precursor conversion and crystallization control otherwise demanded from the deposition step.

The temperature at which this recrystallization is induced plays a key role, as it has been shown to yield control over the morphological grain size of the resulting $MAPbI_3$ film, allowing to tune it over several orders of

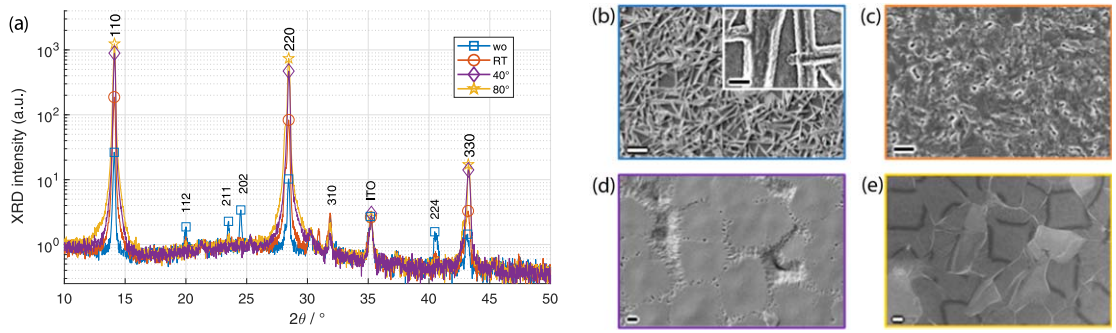

Figure 2. (a) XRD spectra and (b)–(e) SEM images of pristine and MA-treated $MAPbI_3$ films: (b) without MA treatment; MA-treated and recrystallized at (c) room temperature, (d) 40 °C, and (e) 80 °C. Black scale bars denote 1 μm, white ones 10 μm.

magnitude [16]. Figure 2 demonstrates the wide range accessible with this approach, expanding the diameter from few hundred nm at room temperature (figure 2(c)) to many tens of μm when the films are recrystallized on a hotplate at 80 °C (figure 2(e)). While one has to be careful with the distinction between grains as apparent in e.g. scanning electron microscopy, and monocrystalline domains in the sense of undisturbed periodic lattice arrangement as determined by high-resolution transmission electron microscopy or analysis of x-ray diffraction data, since they need not coincide [14, 15, 17], the former was found to be decisive for charge transport and thus device performance [14, 18].

Furthermore, XRD shows a preferential alignment of the recrystallized perovskite along the (110) orientation with the corresponding diffraction peaks increasing manifold in the MA treated films, whereas all other previously detectable orientations vanish (figure 2(a)). This highly oriented (110) arrangement is a common factor (albeit to varying degrees) to various MA based techniques [9, 15, 17], and has previously been related to improved device performance [19, 20].

3. Stability benefits

Associated with the morphological improvements realized by the MA method comes the additional advantage of enhanced stability against degradation. The reason for this can be argued to be twofold:

On the one hand, the tunability of the grain size equivalently influences the relative occurrence of grain boundaries which is, quite evidently, reduced in films with larger grains. Grain boundaries in $MAPbI_3$ films have been shown to be the primary point of attack for temperature [21], moisture [22], and oxygen [23] related degradation, with the decomposition of the perovskite starting at the grain boundaries and progressing inwards from there in plane (figures 3(a)–(g)). This has been related to the amorphous nature of the grain boundary region [22], acting as a crystallographic weak spot, while also providing an increased surface area compared to a compact film. As a consequence, larger grains are directly correlated not only with cell performance [24], but also cell stability [25]. These observations are consistent with the fact that macroscopic $MAPbI_3$ perovskite single crystals have been found to be stable in ambient air for years [22].

On the other hand, the crystallinity of the grain boundaries itself is also amenable to MA treatment. Similar to the above mentioned detrimental gaseous influences, access to the bulk is assumed to equally take place predominantly via the grain boundaries for the MA molecules. Correspondingly, Jiang *et al* report to have 'fused' grain boundaries by means of their MA treatment, while maintaining the same morphological grain size as the reference. The thus modified cells have proven to sustain their initial PCE longer during maximum power point tracking, i.e. under continuous illumination and electrical load, at ambient conditions [26] (figures 3(h), (i)).

Notably, MA induced recrystallization has also been successfully applied to the entire cell stack, to repeatedly recover device performance after photo-degrading the cell at elevated temperatures [27].

4. Applicability and perspectives

While various other fabrication methods for organic–inorganic halide perovskite films and solar cells have been developed in a laboratory environment with good results, the ultimate goal of all these efforts is to eventually apply industrially produced modules on a large scale. It has proven challenging to produce working devices with an area of significantly more than 1 cm^2 while maintaining high film quality and adequate device performance [28–30]. The solution-processing protocols that were so carefully developed for laboratory-scale devices are

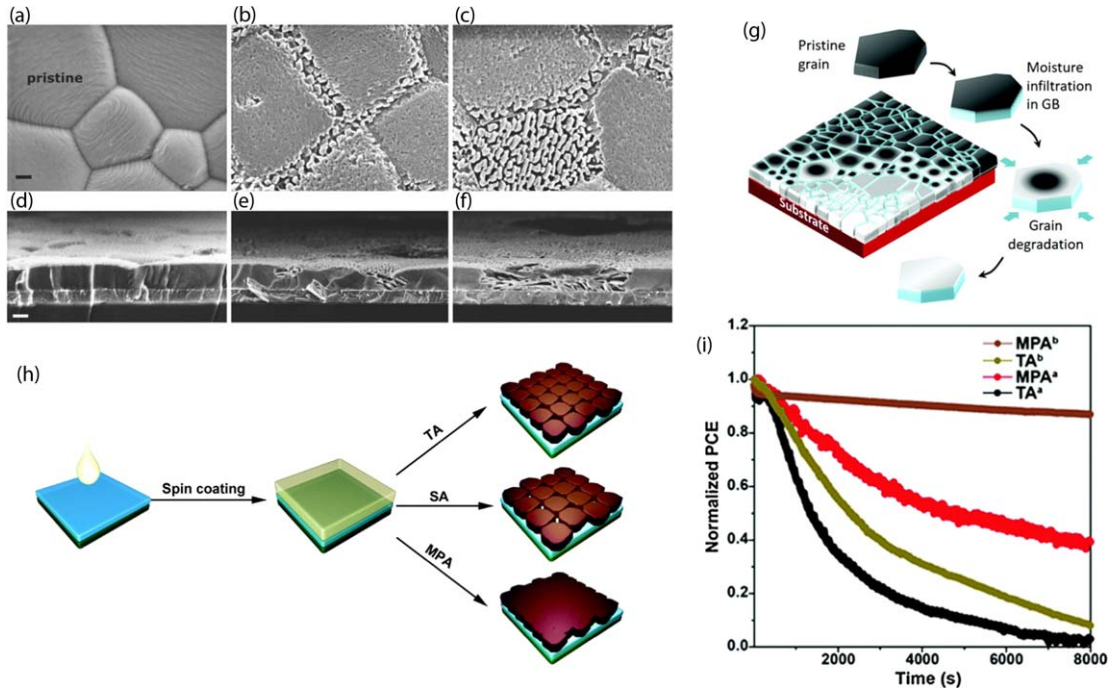

Figure 3. (a)–(f) SEM images documenting the progressing oxygen related degradation of $MAPbI_3$, scale bars 200 nm, reproduced with permission from Wiley [23]. (g) Illustration of the process of moisture related degradation via grain boundaries, reproduced with permission from the Royal Society of Chemistry [22]. (h) Schematic of the resulting film morphologies from thermal annealing (TA), solvent annealing (SA), and methylamine post-annealing (MPA), (i) the corresponding MPP tracking data of planar[a] and mesoporous[b] devices at 50% relative humidity, reproduced from [26] published by the Royal Society of Chemistry.

mostly not easily adapted for larger areas, where they result in poorer quality films with pinholes and insufficient uniformity [4, 31, 32].

MA gas treatments hold an immense potential to tackle these problems and greatly benefit progress in upscaling towards industrial employment [33]. Owing to its ability of yielding a smooth, pinhole-free perovskite layer regardless of the morphology of the original film, relatively poor quality perovskite layers, readily obtainable on large areas by blade or slot-dye coating, could be transformed into highly crystalline, large-grained films. With further investigations as to the precise influence of process parameters such as MA partial pressure, temperature, and exposure time, the morphology of such films could be adjusted to accommodate various demands for different applications.

An important aspect to be considered, both with regards to technical implementation as well as cell architecture, is the corrosive nature of MA. Apart from the desired interaction with the perovskite layer, unwanted chemical interference with processing equipment and subajacent layers in the cell stack alike have to be prevented. This mainly presents a challenge where organic charge selective layers or surface modifiers are employed beneath the perovskite, as they can often be primarily subjected to detriment brought about by the chemical reactivity of MA [34]. Therefore, we expect progress in optimizing interfacial processes between perovskite and inorganic charge selective layers without relying on organic compounds to fully unlock the potential of MA treatment for high-efficiency PSCs.

Besides the adjacent layers, a move towards an all-inorganic composition also of the perovskite itself is subject of extensive research, since it promises inherently improved stability [35]. Despite being based on the interaction of MA with $MAPbI_3$, the MA recrystallization method has already been shown to work on all-inorganic perovskite materials as well. Recently, a uniform inorganic cesium-based perovskite layer ($CsPbX_3$) with high crystallinity was formed by adding sacrificial methylammonium halide (MAX) to $CsPbX_3$ precursor films, facilitating the liquid intermediate state that is also observed during the treatment of $MAPbI_3$ films. Upon recrystallization, the methylammonium leaves the perovskite film and a uniform, pin-hole free $CsPbX_3$ perovskite film is achieved [36]. When instead of adding excess MAX, precursor concentrations are kept stochiometric, mixed organic–inorganic cation perovskite can be formed, which can benefit from the morphological improvements of the MA gas post-deposition treatment without exhibiting signs of phase separation or compositional changes, as has been shown for the case of $Cs_xMA_{1-x}PbI_3$ [37].

All-organic mixed cations, most commonly combinations of methylammonium and formamidinium, display a more complex interplay: besides the aforementioned possibility of conversion via the high temperature chemical redox reaction described by Zhou *et al* [10], dependence on MA partial pressure and the polymorphic

nature of $FAPbI_3$ diversify the phase diagrams of the process [13, 38]. E.g. Zhang and coworkers discovered a phase separation of δ-$FAPbI_3$ and $MAPbI_3$ upon MA exposure of $FA_xMA_{1-x}PbI_3$, passivating and stabilizing the film and the resulting devices [39].

For even more variegated compounds, such as triple or quadruple cation perovskites, predictions regarding the exact effects of MA-induced recrystallization on phase homogeneity and composition still lack substantiated experimental or calculational evidence. However, based on groundwork concerning organic cationic exchange mechanisms [11, 40] and gas-based tuning of mixed halides [7], we are confident that the post-processing and/or fabrication of well-defined multi-compound perovskite materials in both the A as well as the X site should be possible by appropriate protocols, while at the same time exploiting the benefits of the recrystallization process on morphology and stability.

Furthermore, the capability to substantially enhance grain size opens a range of new possibilites for PSCs, such as back-contacted device architectures. For the common planar type architecture, where a perovskite layer of a few hundred nm thickness is sandwiched between charge selective layers, grain sizes on that same length scale are usually sufficient to span both electrodes to ensure unhindered charge transport. When, however, the hunt for record efficiencies moves perovskite research towards back-contacted architectures as it has for conventional photovoltaics, the superior lateral conductivity of grains bridging many micrometers between electrodes may become essential for efficient charge extraction [15, 41, 42].

5. Conclusion

Methylamine gas treatments offer the prospect of post-deposition control over the morphology and grain size in perovskite films. Grain size can be significantly increased, reducing degradation-prone grain boundaries and thus improving device stability. Until now, a wide variety of implementations have adumbrated the range of possibilities this versatile gas–solid interaction has opened up. While surely many more will follow, a focus of onward investigations should lie in determining the intricate details of the recrystallization step and developing a unified protocol of relevant experimental parameters to control and report. More fundamental research seems necessary to fully control the crystal growth, inducing growth in specific directions and eventually forming single crystalline films. Whether e.g. seeding the growth by locally triggering the crystallization will lead to improved film quality still needs to be proven. This understanding will enable investigating in detail the effect of grain boundaries on device performance and stability, including the effect on charge carrier dynamics and transport.

As a comparably easily up-scalable technique, with an improved understanding of the parameter space this method holds the prospects for transforming high-quality perovskite film formation from a fragile laboratory art form into a reliable industrial process.

Acknowledgments

The authors acknowledge the German Research Foundation (DFG) for funding via the priority program SPP2196. ERS acknowledges support by the Stiftung Industrieforschung through a graduate scholarship. CE and TS thank Tom Kollek for kind assistance with XRD measurements.

ORCID iDs

Lukas Schmidt-Mende https://orcid.org/0000-0001-6867-443X

References

[1] REN21 2019 Renewables 2019 global status report *Technical Report* REN21
[2] Kojima A, Teshima K, Shirai Y and Miyasaka T 2009 *J. Am. Chem. Soc.* **131** 6050–1
[3] NREL 2019 Research-cell efficiency chart (https://nrel.gov/pv/cell-efficiency.html)
[4] Rong Y, Hu Y, Mei A, Tan H, Saidaminov M I, Seok S I, McGehee M D, Sargent E H and Han H 2018 *Science* **361** eaat8235
[5] Li Y, Ji L, Liu R, Zhang C, Mak C H, Zou X, Shen H H, Leu S Y and Hsu H Y 2018 *J. Mater. Chem.* A **6** 12842–75
[6] Zhou Z, Wang Z, Zhou Y, Pang S, Wang D, Xu H, Liu Z, Padture N P and Cui G 2015 *Angew. Chem., Int. Ed.* **54** 9705–9
[7] Raga S R, Ono L K and Qi Y 2016 *J. Mater. Chem.* A **4** 2494–500
[8] Pang S, Zhou Y, Wang Z, Yang M, Krause A R, Zhou Z, Zhu K, Padture N P and Cui G 2016 *J. Am. Chem. Soc.* **138** 750–3
[9] Long M *et al* 2017 *Nano Energy* **33** 485–96
[10] Zhou Y, Yang M, Pang S, Zhu K and Padture N P 2016 *J. Am. Chem. Soc.* **138** 5535–8
[11] Yang J, Qin T, Xie L, Liao K, Li T and Hao F 2019 *J. Mater. Chem.* C **7** 10724–42
[12] Raga S R, Jiang Y, Ono L K and Qi Y 2017 *Energy Technol.* **5** 1750–61
[13] Zhao T, Williams S T, Chueh C C, deQuilettes D W, Liang P W, Ginger D S and Jen A K Y 2016 *RSC Adv.* **6** 27475–84

[14] Conings B, Bretschneider S A, Babayigit A, Gauquelin N, Cardinaletti I, Manca J, Verbeeck J, Snaith H J and Boyen H G 2017 *ACS Appl. Mater. Interfaces* **9** 8092–9
[15] Zhang M J, Wang N, Pang S P, Lv Q, Huang C S, Zhou Z M and Ji F X 2016 *ACS Appl. Mater. Interfaces* **8** 31413–8
[16] Jacobs D L and Zang L 2016 *Chem. Commun.* **52** 10743–6
[17] Jiang Y, Tu L, Li H, Li S, Yang S E and Chen Y 2018 *Crystals* **8** 44
[18] Reid O G, Yang M, Kopidakis N, Zhu K and Rumbles G 2016 *ACS Energy Lett.* **1** 561–5
[19] Lian J, Wang Q, Yuan Y, Shao Y and Huang J 2015 *J. Mater. Chem.* A **3** 9146–51
[20] Docampo P, Hanusch F C, Giesbrecht N, Angloher P, Ivanova A and Bein T 2014 *APL Mater.* **2** 081508
[21] Yang R *et al* 2019 *IEEE J. Photovolt.* **9** 207–13
[22] Wang Q, Chen B, Liu Y, Deng Y, Bai Y, Dong Q and Huang J 2017 *Energy Environ. Sci.* **10** 516–22
[23] Sun Q, Fassl P, Becker-Koch D, Bausch A, Rivkin B, Bai S, Hopkinson P E, Snaith H J and Vaynzof Y 2017 *Adv. Energy Mater.* **7** 1700977
[24] Nie W *et al* 2015 *Science* **347** 522–5
[25] Chiang C H and Wu C G 2016 *ChemSusChem* **9** 2666–72
[26] Jiang Y, Juarez-Perez E J, Ge Q, Wang S, Leyden M R, Ono L K, Raga S R, Hu J and Qi Y 2016 *Mater. Horiz.* **3** 548–55
[27] Hong L, Hu Y, Mei A, Sheng Y, Jiang P, Tian C, Rong Y and Han H 2017 *Adv. Funct. Mater.* **27** 1703060
[28] Chen W *et al* 2015 *Science* **350** 944–8
[29] Qiu W *et al* 2016 *Energy Environ. Sci.* **9** 484–9
[30] Seo J, Park S, Chan Kim Y, Jeon N J, Noh J H, Yoon S C and Seok S I 2014 *Energy Environ. Sci.* **7** 2642–6
[31] Razza S, Castro-Hermosa S, Di Carlo A and Brown T M 2016 *APL Mater.* **4** 091508
[32] Wang F, Cao Y, Chen C, Chen Q, Wu X, Li X, Qin T and Huang W 2018 *Adv. Funct. Mater.* **28** 1803753
[33] Li C, Pang S, Xu H and Cui G 2017 *Sol. RRL* **1** 1700076
[34] Liu T, Jiang F, Tong J, Qin F, Meng W, Jiang Y, Li Z and Zhou Y 2016 *J. Mater. Chem.* A **4** 4305–11
[35] Li B, Fu L, Li S, Li H, Pan L, Wang L, Chang B and Yin L 2019 *J. Mater. Chem.* A **7** 20494–518
[36] Shao Z, Wang Z, Li Z, Fan Y, Meng H, Liu R, Wang Y, Hagfeldt A, Cui G and Pang S 2019 *Angew. Chem., Int. Ed.* **58** 5587–91
[37] Chang Y, Wang L, Zhang J, Zhou Z, Li C, Chen B, Etgar L, Cui G and Pang S 2017 *J. Mater. Chem.* A **5** 4803–8
[38] Li C, Zhou Y, Wang L, Chang Y, Zong Y, Etgar L, Cui G, Padture N P and Pang S 2017 *Angew. Chem., Int. Ed.* **56** 7674–8
[39] Zhang Y, Zhou Z, Ji F, Li Z, Cui G, Gao P, Oveisi E, Nazeeruddin M K and Pang S 2018 *Adv. Mater.* **30** 1707143
[40] Wang J *et al* 2018 *Sol. RRL* **2** 1800125
[41] Lin X, Chesman A S R, Raga S R, Scully A D, Jiang L, Tan B, Lu J, Cheng Y B and Bach U 2018 *Adv. Funct. Mater.* **28** 1805098
[42] Hou Q *et al* 2018 *Nano Energy* **50** 710–6